Journal of Cleaner Production 382 (2023) 135290

Contents lists available at ScienceDirect

Journal of Cleaner Production

journal homepage: www.elsevier.com/locate/jclepro

The effect of climate and vegetation variation on monthly sediment load in a karst watershed

Si Cheng [a], Xingxiu Yu [a], Zhenwei Li [b,c,d,*], Xianli Xu [b,c,d], Huayi Gao [e], Zongda Ye [f,g]

[a] Faculty of Resources and Environmental Science, Hubei University, Wuhan, 430062, China
[b] Huanjiang Observation and Research Station for Karst Ecosystem, Key Laboratory for Agro-Ecological Processes in Subtropical Region, Institute of Subtropical Agriculture, Chinese Academy of Sciences, Changsha, 410125, China
[c] Guangxi Key Laboratory of Karst Ecological Processes and Services, Huanjiang, 547100, China
[d] Institutional Center for Shared Technologies and Facilities of Institute of Subtropical Agriculture, Chinese Academy of Sciences, Changsha, 410125, China
[e] Yangtze University School of Geosciences, Wuhan, 430100, China
[f] Natural Resources Ecological Restoration Center of Guangxi Zhuang Autonomous Region, Nanning, 530000, China
[g] Technical Innovation Center of Mine Geological Environmental Restoration Engineering in Southern Karst Area, Ministry of Natural Resources, Nanning, 530000, China

ARTICLE INFO

Keywords:
Climate change
Vegetation dynamics
Monthly sediment load
Partial least squares-structural equation modeling
Karst ecosystems

ABSTRACT

The variation in monthly sediment load is greatly influenced by climate and vegetation changes which are generally coupled and interconnected. However, few studies have quantified the relative magnitudes of the direct and indirect influences of climate variability and vegetation dynamics on monthly sediment load. The objective of this study was to decouple the impacts of climate and vegetation changes on the monthly sediment load in a karst watershed using partial least squares-structural equation modeling (PLS-SEM). Monthly sediment load, runoff, climatic factors (temperature and precipitation), and vegetation data (NDVI, EVI, and LAI) were collected from 2003 to 2017. Results indicated that climatic factors and vegetation dynamics explained 73% of the variation in monthly runoff, while climatic factors, vegetation dynamics, and runoff accounted for 62% of the monthly sediment load changes. Climate change can not only directly alter vegetation and hydrological characteristics, but also indirectly affect hydrological characteristics by changing vegetation dynamics, thus affecting the cooperative processes of runoff and sediment load. Specifically, runoff (direct effect = 0.84) and precipitation (indirect effect = 0.67) had a positive impact on monthly sediment load, while antecedent temperature (indirect effect = −0.02), temperature (indirect effect = −0.03), antecedent precipitation (indirect effect = −0.01), and vegetation dynamics (direct effect = −0.12; indirect effect = 0.07) had a negative impact. Compared with traditional methods, PLS-SEM can more completely describe the relationship among the observed variables and other potential influencing variables and may provide relevant references for eco-hydrological management and land resource optimization in karst watersheds.

1. Introduction

Soil erosion can lead to land degradation and even local environmental degradation ({Fu, 1994 #48;Syvitski, 2005 #41}Syvitski et al., 2005; Wang et al., 2015; Borrelli et al., 2020). Sediment transport, a significant component of soil erosion, is greatly influenced by topography, geology, watershed area, land cover and climate (Marques et al., 2007; Wei et al., 2007; Wang et al., 2013). For a specific watershed, the topographical and geological conditions and watershed area remain relatively invariable in the short term (e.g., several decades), while the vegetation cover and climatic factors show significant temporal variation (Shi et al., 2014; Zhang et al., 2021). Changes in vegetation cover can considerably affect the generation and intensity of runoff and sediment load in a watershed (Karvonen et al., 1999; Chen et al., 2003; Xu et al., 2008; Gao et al., 2017). For example, as vegetation coverage increases significantly, it becomes the most important factor affecting the intensity and frequency of soil erosion in the Loess Plateau (Gao et al., 2012; Wang et al., 2015). Similarly, climatic factors such as

* Corresponding author. Huanjiang Observation and Research Station for Karst Ecosystem, Key Laboratory for Agro-Ecological Processes in Subtropical Region, Institute of Subtropical Agriculture, Chinese Academy of Sciences, Changsha, 410125, China.
E-mail addresses: 1073204744@qq.com (S. Cheng), xxy2000@126.com (X. Yu), lizhenwei337@isa.ac.cn (Z. Li), xianlixu@isa.ac.cn (X. Xu), 471986089@qq.com (H. Gao), 598474889@qq.com (Z. Ye).

https://doi.org/10.1016/j.jclepro.2022.135290
Received 17 July 2022; Received in revised form 7 November 2022; Accepted 21 November 2022
Available online 25 November 2022

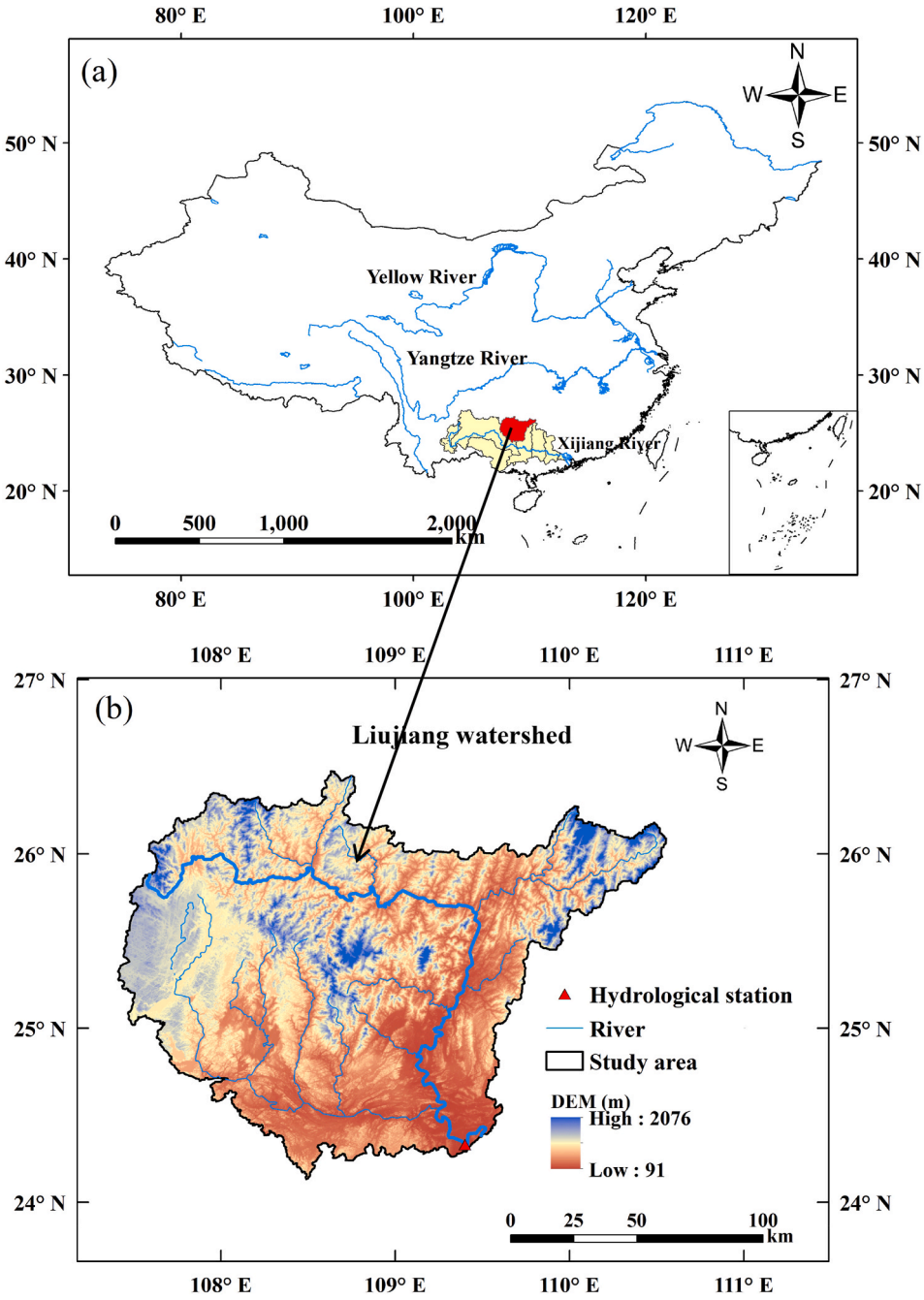

Fig. 1. Location of the Liujiang watershed and hydrological station in the karst region of southwest China, including the digital elevation model (DEM), with black lines showing the watershed boundaries.

temperature and precipitation also have significant temporal and spatial variability, which further affect the runoff and sediment load (Yan et al., 2013). Furthermore, temperature and precipitation play an important role in vegetation dynamics, and thus exert substantial influence on runoff and sediment load changes in a watershed (Lin et al., 1996; Li et al., 2015; Serpa et al., 2015; Liu et al., 2022). Antecedent precipitation and temperature are also closely related to vegetation dynamics and, hence, runoff and sediment load (Seeger et al., 2004). These complex relationships are likely to hinder a comprehensive understanding of sediment transport processes in response to climate variability and vegetation dynamics. Therefore, to evaluate the impact of climate change on runoff and sediment load, it is crucial to quantify not only its direct impacts, but also its indirect influences on runoff and sediment load by effecting vegetation.

With respect to the importance of climate change and vegetation dynamics on runoff or sediment load, previous studies were largely concerned with annual scales, and likely neglected seasonal variations in sediment load (Wei et al., 2007; Zhao et al., 2010; Shi et al., 2014; Zhou et al., 2015; Mwangi et al., 2016; Feng et al., 2016; Zhang et al., 2019). Some studies have found that sediment load changes are more obvious on a monthly scale than on an annual scale, and hence, the driving forces affecting monthly sediment load can be better identified (Chen et al., 2001; Zhang and Lu, 2009). Furthermore, the relationship between monthly sediment load and its influencing factors is relatively complicated and worthy of further exploration.

Runoff generation and sediment transport processes are non-stationary and variable, and have complex responses to the climate

Table 1
Abbreviations and descriptions of the monthly sediment load and its potential influencing variables in a typical karst watershed.

Variables	Abbreviations	Unit	Description
Antecedent Temperature	1. T1mon	°C	Monthly average temperature 1 month before
	2. T2mon	°C	Monthly average temperature 2 months before
	3. T3mon	°C	Monthly average temperature 3 months before
Temperature	4. T	°C	Monthly average temperature
	5. T_{max}	°C	Monthly maximum temperature
	6. T_{min}	°C	Monthly minimum temperature
Antecedent Precipitation	7. P1mon	mm	Monthly total precipitation 1 month before
	8. P2mon	mm	Monthly total precipitation 2 months before
	9. P3mon	mm	Monthly total precipitation 3 months before
Precipitation	10. P_{tot}	mm	Monthly total precipitation
	11. PD	–	Monthly number of days with precipitation >0.1 mm
	12. P1day	mm	Monthly maximum 1-day precipitation
	13. P3day	mm	Monthly maximum 3-day precipitation
	14. P7day	mm	Monthly maximum 7-day precipitation
Runoff	15. Q	10^8 m^3 s^{-1}	Monthly total discharge
Sediment load	16. SL	10^4 t	Total sediment load
Vegetation	17. NDVI	–	Normalized difference vegetation index
	18. EVI	–	Enhanced vegetation index
	19. LAI	–	Leaf area index

and underlying surfaces (Sivapalan et al., 2001; Pruski and Nearing, 2002; Vercruysse et al., 2017). In general, the methods used to isolate the impact of climate change and vegetation dynamics on watershed runoff are well developed. Empirical statistics (e.g., simple linear regression, double mass curve, sediment identify factor analysis, and elastic coefficient method) or distributed hydrological models (DHMs) (e.g., Sediment Delivery Distributed (SEDD) and Soil and Water Assessment Tool (SWAT) models) have been used to investigate the responses of sediment load to climate change and vegetation dynamics (Miao et al., 2011; Zhang et al., 2019). For example, Serpa et al. (2015) used the SWAT model to separate the impact of climate and land use change on runoff and sediment load in both wet and dry Mediterranean watersheds, and found that climate change would reduce runoff in both watersheds, while sediment load decreased only in the humid watershed. Zhang et al. (2019) established a regression model between the climatic factors and normalized difference vegetation index (NDVI) to evaluate the synergistic effects of annual precipitation and temperature on sediment yield changes in the Jinshajiang River watershed. However, the climatic and vegetation variables are generally considered to be independent in these methods. As a result, the empirical statistics and DHMs struggle to perform accurate quantitative analyses of the relationships among latent variables. Therefore, these methods cannot effectively distinguish the direct and indirect effects of climate change and vegetation dynamics on the hydrological characteristics of watersheds.

Recently, the structural equation model (SEM) has been used to resolve the relationship between an independent variable and a dependent variable, which is direct influence, and the relationship between an independent variable and a dependent variable that is transmitted by a medium, which is indirect influence (Vinzi et al., 2010). Thus, through a theoretical model based on certain assumptions, each latent variable can be obtained from observable variables (Pearl, 2012; Grace et al., 2012). Compared with traditional statistical analysis

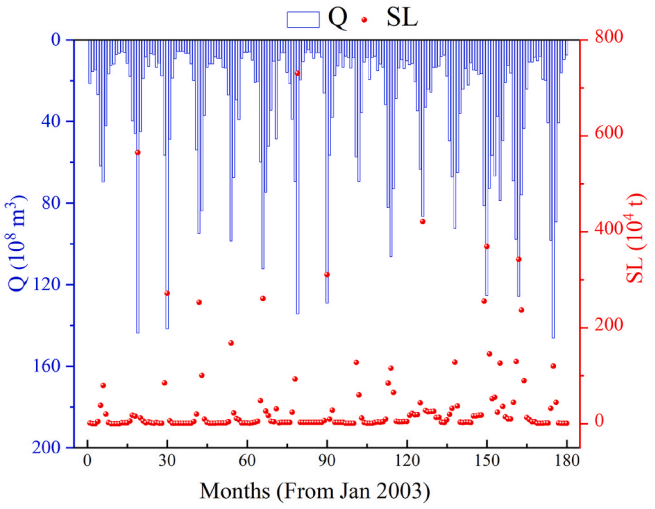

Fig. 2. Temporal variations in monthly runoff (Q) and sediment load (SL) in the Liujiang watershed from January 2003 to December 2017.

Table 2
Descriptive statistics of the monthly sediment load and its potential influencing variables in the Liujiang watershed from 2003 to 2017.

Variables		Minimum	Maximum	Median	Mean	S.D	CV (%)
AntecedentTemperature	T1mon	3.9	28.7	20.5	19.1	6.8	35.6
	T2mon	3.9	28.7	20.5	19.1	6.8	35.6
	T3mon	3.9	28.7	20.5	19.1	6.8	35.6
Temperature	T	3.9	28.7	20.5	19.1	6.8	35.6
	T_{max}	8.4	30.9	26.1	24.4	5.5	22.5
	T_{min}	−0.7	25.9	14.1	13.7	7.7	56.2
Antecedent Precipitation	P1mon	2.3	371.3	87.6	112.6	81.7	72.6
	P2mon	2.3	371.3	87.6	112.4	81.8	72.8
	P3mon	2.3	371.3	88.5	112.9	81.8	72.5
Precipitation	P_{tot}	2.3	371.3	87.1	112.2	81.9	73.0
	PD	1.0	23.6	12.0	11.9	4.5	37.8
	P1day	1.6	73.2	32.3	34.1	18.5	54.3
	P3day	2.3	171.8	61.7	70.4	42.6	60.5
	P7day	2.3	290.5	81.1	99.3	67.3	67.8
Runoff	Q	4.8	146.3	17.3	32.9	33.1	100.6
Sediment Load	SL	0.0	730.7	4.1	39.5	96.3	243.9
Vegetation	NDVI	0.1	0.8	0.7	0.6	0.1	16.7
	EVI	0.1	0.8	0.4	0.4	0.1	25.0
	LAI	0.4	5.6	3.0	3.0	1.3	43.3

S.D: standard deviation; CV: coefficient of variation. Abbreviations for the variables are listed in Table 1.

Table 3
Summary of the trend analysis for monthly runoff and sediment load during 2003–2017 using the Mann-Kendall Test.

Time series Latent Variables	Runoff			Sediment load		
	Z	P	Trend	Z	P	Trend
Jan	1.78	0.07	Increasing	1.73	0.08	Increasing
Feb	0.45	0.66	Increasing	2.03	**0.04**	**Increasing**
Mar	1.88	0.06	Increasing	2.33	**0.02**	**Increasing**
Apr	1.09	0.28	Increasing	1.59	0.11	Increasing
May	1.58	0.11	Increasing	0.79	0.43	Increasing
Jun	0.99	0.32	Increasing	0.89	0.37	Increasing
Jul	0.40	0.69	Increasing	1.39	0.17	Increasing
Aug	1.58	0.11	Increasing	2.18	**0.03**	**Increasing**
Sep	1.68	0.09	Increasing	0.94	0.35	Increasing
Oct	2.28	**0.02**	**Increasing**	2.13	**0.03**	**Increasing**
Nov	1.39	0.17	Increasing	1.54	0.12	Increasing
Dec	2.08	**0.04**	**Increasing**	2.53	**0.01**	**Increasing**

Bold number indicates significant trends at 95% confidence level.

methods, SEM can clearly express the relationships within structures represented by multiple variables. The partial least squares (PLS) method based on SEM, also known as PLS Path Modeling (PLS-PM) can explain residual variances in latent variables and manifest variables in model regression operations (Vinzi et al., 2010). Partial least squares structural equation modelling (PLS-SEM) can combine measurement and structural models to construct a conceptual model of the relationships among independent variables and dependent variables. This method has low requirements for sample size and mainly produces optimal predictions for results (Tenenhaus et al., 2005; Tenenhaus, 2008; Vinzi et al., 2010). Few studies, however, have used PLS-SEM to decouple the influences of climate change and vegetation dynamics on monthly sediment load, especially in karst landscape where an ecologically vulnerable area experiencing severe soil erosion.

The karst region of southwest China is one of the largest continuous karst regions in the world, with approximately 510000 km^2 of highly irregular exposed carbonate rocks (Jiang et al., 2014; Hartmann et al., 2014). This ecologically fragile area has serious soil erosion (Feng et al.,

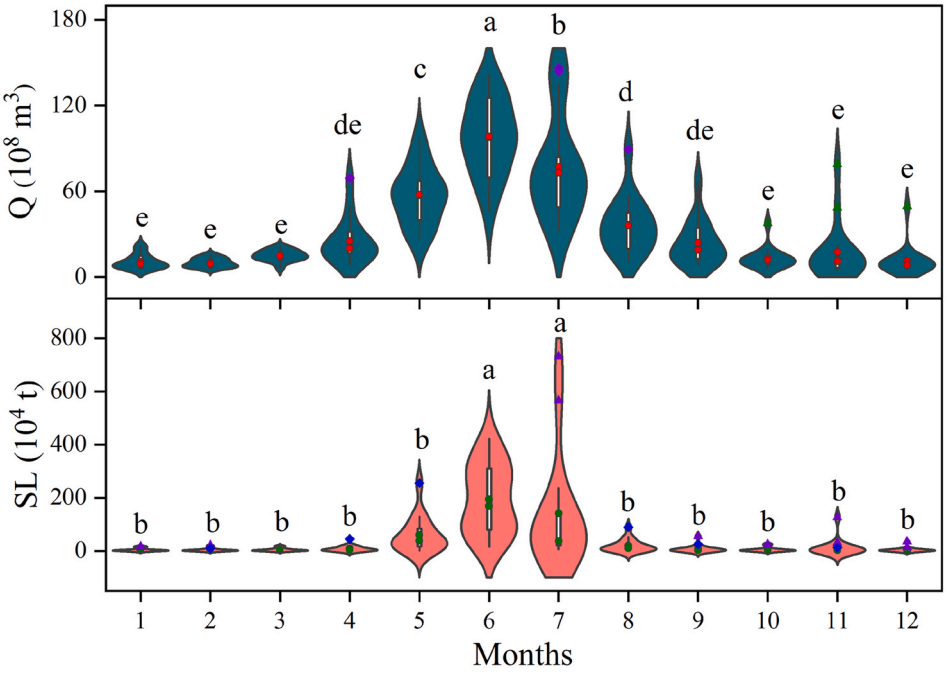

Fig. 3. Comparisons of the monthly runoff (Q) and sediment load (SL) among different months using data from the 2003–2017 observation period. The red circle shows the median, the purple diamond displays the outliers, the red square represents the average, and the green triangle shows the extreme value. Different letters indicate significant differences at $P < 0.05$ among different months.

Table 4
Comparisons of temperature, precipitation, and vegetation variables among different months during 2003–2017.

LV	AOV	Month											
		Jan	Feb	Mar	Apr	May	Jun	Jul	Aug	Sep	Oct	Nov	Dec
Temperature	T	8.2j	11.0i	14.3h	19.8f	23.4d	25.9b	27.6a	27.3a	24.9c	20.8e	15.6g	10.3i
	T_{max}	15.1g	20.0f	22.2e	26.6d	28.2c	29.3abc	30.1a	29.9 ab	28.5bc	25.3d	22.1e	15.8g
	T_{min}	2.7j	4.4i	7.1h	12.5f	18.4d	21.9b	24.5a	23.1b	20.0c	15.2e	9.7g	5.5i
Precipitation	P_{tot}	46.8h	45.2h	83.9 fg	123.1de	215.3b	261.6a	165.3c	138.4cd	95.9ef	57.3gh	71.6fgh	42.0h
	PD	10.6de	10.5de	15.3 ab	14.3abc	15.9 ab	16.8a	13.6bc	12.4cd	9.2ef	6.9f	9.4ef	8.2ef
	P1day	19.5g	16.0g	24.4 fg	36.2de	55.5 ab	61.3a	47.6bc	41.0cd	38.3de	23.2 fg	29.5ef	17.4g
	P3day	34.8ef	30.6f	50.4ef	77.0c	123.3a	140.6a	99.4b	86.6bc	71.7cd	44.2ef	54.2de	32.5f
	P7day	43.7gh	41.1h	72.1 fg	107.8de	185.3b	218.6a	144.0c	124.4cd	91.5ef	55.1gh	68.0fgh	40.2h
Vegetation	NDVI	0.5g	0.5 fg	0.5f	0.7de	0.7bcd	0.7cde	0.7 ab	0.8a	0.8a	0.7abc	0.7cde	0.6e
	EVI	0.2gh	0.2h	0.3 fg	0.4de	0.4c	0.5bc	0.5a	0.5 ab	0.5bc	0.4d	0.3e	0.3f
	LAI	1.4e	1.7de	1.7de	2.8c	4.0b	3.2c	4.4 ab	4.5a	4.3 ab	3.3c	2.9c	2.0d

Different letters indicate significant differences at $P < 0.05$ among different months.

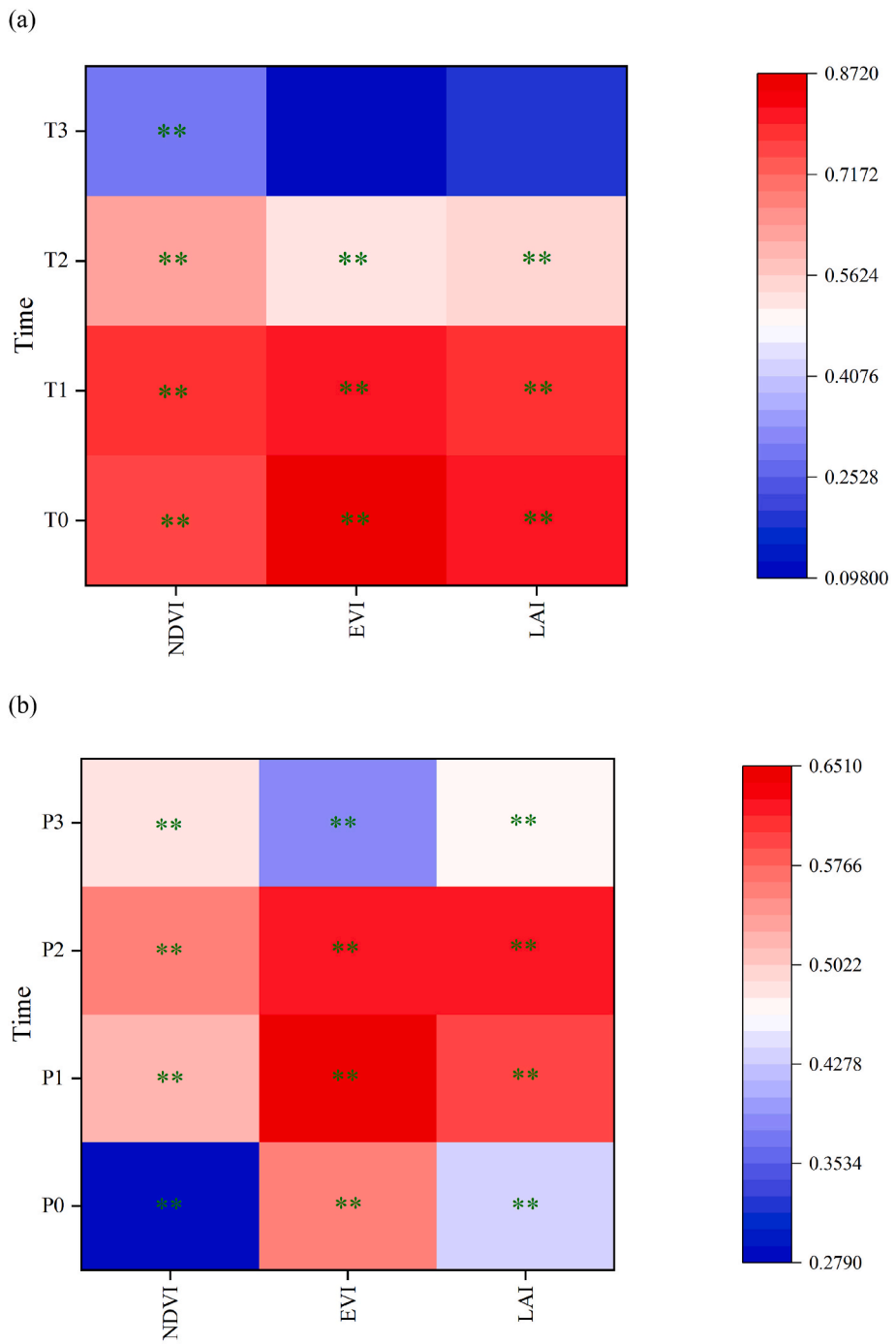

Fig. 4. Thermal maps of Pearson correlation coefficients between vegetation index and (a) temperature and (b) precipitation with different lag times (0–3 months). * and ** indicate significance at $P < 0.05$ and $P < 0.01$, respectively. Abbreviations for the variables are listed in Table 1.

2016; Li et al., 2016). Typically, precipitation that falls on hillsides quickly drains underground through numerous fissures and cracks, replenishing groundwater systems (Li et al., 2019). As a result, the proportion of surface runoff from precipitation is much lower than that in non-karst watersheds (Zhang et al., 2014). Surface runoff may occur only when precipitation is greater than 60 mm (Peng and Wang, 2012; Hartmann et al., 2014; Li et al., 2017a). Karst areas are characterized by thin surface soil, special lithological conditions, and strong infiltration capacity, which affect the hydrological processes and sediment load (Li et al., 2017b). Consequently, understanding the relationship between climate, vegetation dynamics, and monthly sediment load under these unique geological conditions is crucial to effectively control sediment loads in karst watersheds. However, few studies have decoupled the influences of climate variability and vegetation dynamics on sediment load variation, as well interactive effects among driving factors in karst areas.

The objectives of this study were to investigate the temporal variation in monthly sediment load and its potential influencing factors and to further quantify the contributions of climate, dynamic vegetation factors, and runoff changes to sediment load using the PLS-SEM model in a typical karst watershed in southwest China. Addressing these objectives is expected to provide a more accurate understanding of the hydrological characteristics and a scientific basis for reducing soil erosion and rationally utilizing hydrological resources in karst watersheds under

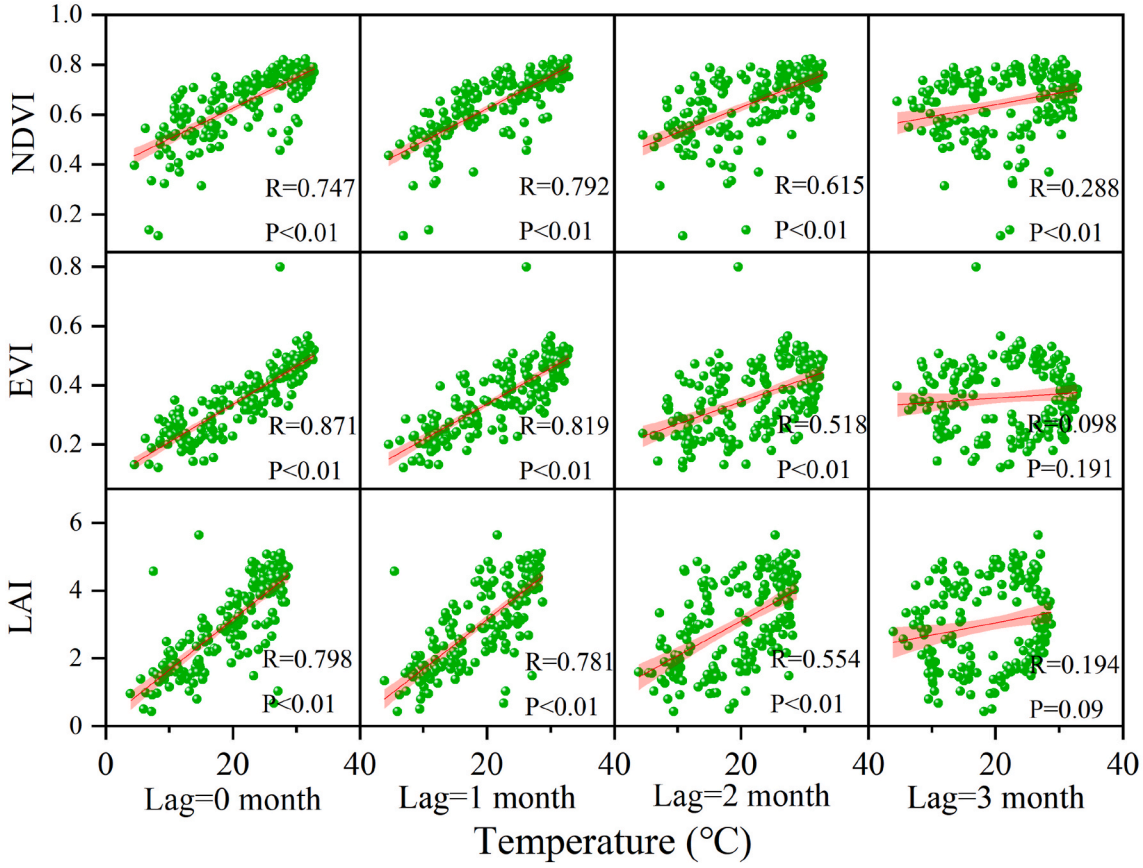

Fig. 5. Scatter plot of the vegetation indexes and temperature in the Liujiang watershed using data from the 2003–2017 observation period.

climate change.

2. Materials and methods

2.1. Study area

The study area is located in the Liujiang watershed (24°8′–26°28′N, 107°24′–110°33′E, 4.54 × 10^4 km^2) in southwest China where the typical karst landscape is widespread (Fig. 1). The Liujiang River is the second largest tributary of the main stream of the Xijiang River in the Pearl River system. It originates in Guizhou, passes through Hunan and Guangxi provinces, and finally joins the Xijiang River at Sanjiang Estuary. Its total length is 773 km. The topography of the Liujiang watershed is characterized by plateaus, mountains, hills, and plains. The elevation ranges from 91 to 2076 m, and the northwest and northeast are higher than the south. The climate is subtropical and tropical monsoon, with the highest precipitation and temperature occurring during the summer. Over the past 50 years, the average annual temperature and precipitation were approximately 18–20 °C and 1400–1800 mm, respectively. The precipitation varies greatly but primarily occurs during the rainy season, from April to August. Woodland is the main land use type. Karst landforms are widely distributed throughout the watershed, and most are soluble carbonate rocks. Due to the special topographic and geological conditions, the soil is weakly resistant to erosion in this region. No large dams have been constructed in the watershed, and thus this region serves as a representative karst area for evaluating the influence of climate and vegetation dynamics on monthly sediment load using the PLS-SEM model (Li et al., 2018).

2.2. Data sources

In this study, climatic factors (monthly temperature and precipitation), monthly runoff, and vegetation characteristics in the Liujiang watershed from 2003 to 2017 were selected as variables that potentially affect monthly sediment load (Table 1). Monthly average temperature, monthly maximum temperature, and monthly minimum temperature were selected to represent the influence of temperature on sediment load. Monthly total precipitation, monthly number of days with precipitation >0.1 mm, monthly maximum 1-day precipitation, monthly maximum 3-day precipitation, and monthly maximum 7-day precipitation were used to reflect the effects of monthly precipitation. The NDVI, enhanced vegetation index (EVI), and leaf area index (LAI) were selected to detect the influence of vegetation. Precipitation and temperature data were obtained from meteorological stations in and around the Liujiang watershed, and monthly scale time series data were provided by meteorological administration in China (https://cdc.nmic.cn/). The monthly runoff and sediment load data were collected at the Liuzhou Hydrological Station and from the Hydrological Yearbook of the Ministry of Water Resources of China. The measurements were conducted at the outlet of the watershed. The relevant datasets were checked to ensure their reliability prior to release. Vegetation data series were obtained from the Moderate Resolution Imaging Spectroradiometer (https://modis.ornl.gov). A digital elevation model with a resolution of 30 m was selected to map the watershed boundary using ArcGIS software (Fig. 1).

2.3. Methods

2.3.1. Statistical analysis

In this study, one-way analysis of variance followed by least significant difference ($P < 0.05$) was used to detect the differences in monthly sediment load, runoff, precipitation, temperature, and vegetation cover among months. The rank-based non-parametric Mann–Kendall trend test was used to detect the trends in monthly sediment load and runoff.

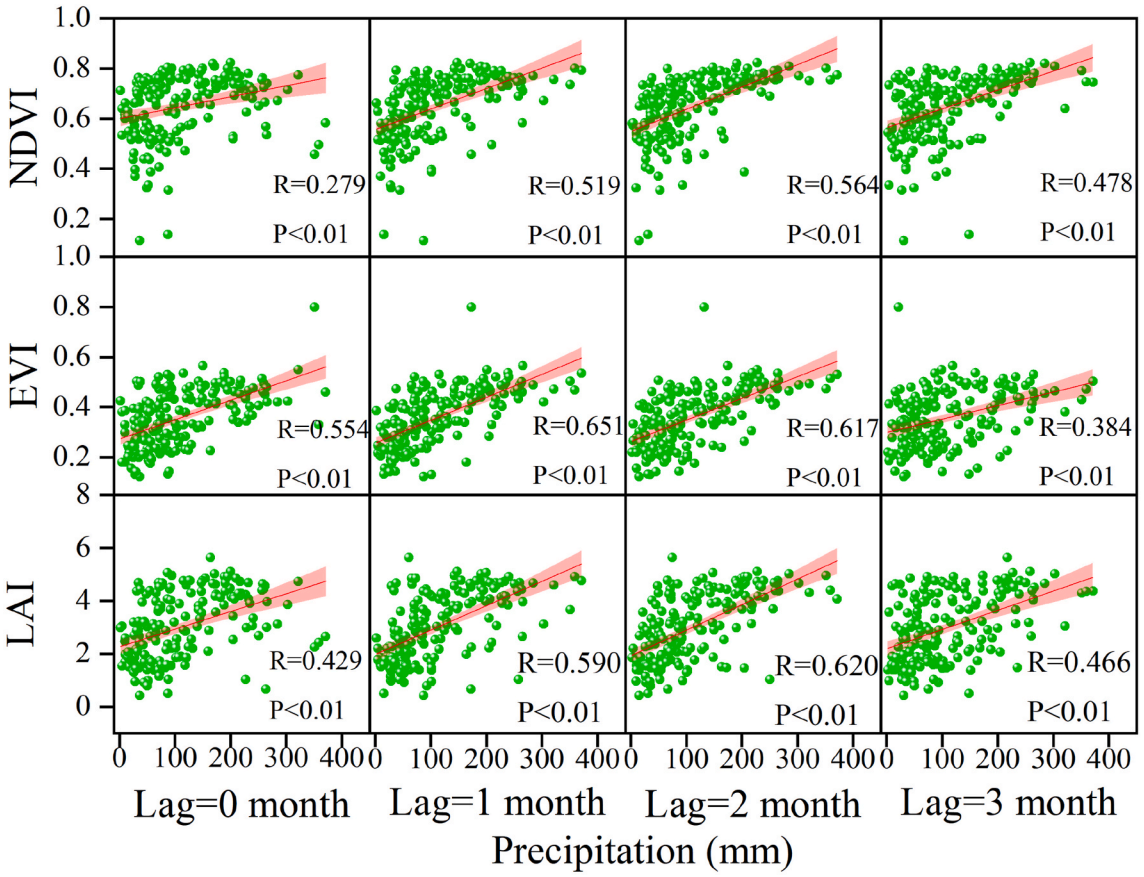

Fig. 6. Scatter plot of the vegetation indexes and precipitation in the Liujiang watershed using data from the 2003–2017 observation period.

Recently, when analyzing the response of vegetation to climate, previous studies have considered the time lag (Wu et al., 2015) that results from temporal variations in vegetation and climate. This relationship was determined using Pearson correlation analysis; the lag period with the highest correlation coefficient (R) indicated the most obvious response of vegetation to climate. Previous studies showed that the response lag time was generally less than 3 months; thus 0–3 lag months between climate change and vegetation response were selected for analysis in this study (Rundquist and Harrington, 2000; Anderson et al., 2010; Saatchi et al., 2013; Chen et al., 2014; Wu et al., 2015).

2.3.2. *Partial least squares-structural equation modeling (PLS-SEM)*

SEM was used to investigate the causal relationship between different latent variables. In a theoretical model based on certain assumptions, the causal relationship between latent variables can be measured using corresponding observable indicators (Vinzi et al., 2010; Grace et al., 2012). SEM model analysis is divided into a measurement model and structural model. The measurement model considers the relationship between each latent variable and the corresponding observable variable, while the structural model solves the complex relationship between latent variables (Vinzi et al., 2010).

PLS-SEM is a component-based estimation method, and is also known as PLS-PM. The components of the measurement model are solved by an iterative algorithm, and then the correlation path coefficients in the structural model are estimated (Tenenhaus, 2008; Vinzi et al., 2010).

The relationship between latent variables (ξ_j) can be expressed as follows:

$$\xi_j = \sum_{i=1}^{i} \beta_{ji}\xi_i + \zeta_j \quad (1)$$

where ξ_j is the general endogenous latent variable, β_{ji} is the path coefficient between the i-th external latent variable and the j-th endogenous latent variable, and ζ_j is the error of the relationship within the model. The relationship between latent variable (ξ_j) and manifest variable (X_{jk}) is expressed as follows:

$$X_{jk} = \lambda_{jk}\xi_j + \varepsilon_{jk} \quad (2)$$

where λ_{jk} is whether the j-th manifest variable is correlated in the k-th block, and the error term ε_{jk} represents the imprecision in measurement (Vinzi et al., 2010). The goodness of fit (*GOF*) index was selected to verify and determine the predictive ability of the model (Tenenhaus et al., 2005; Vinzi et al., 2010), and can be expressed as:

$$GOF = \sqrt{\overline{Communality} \times \overline{R^2}} \quad (3)$$

where *GOF* is the geometric mean of the product of the average community index and the average R^2 value.

In this system, the total effect between two variables is the sum of their direct and indirect effects. The direct effect is determined by the corresponding path coefficient, and the indirect effect refers to the path involving intermediary variables. A conceptual model representing sediment load and climate and vegetation changes in the watershed was constructed, and the climate, vegetation, and hydrological characteristics of the study area were divided into 7 categories (Table 1). In the conceptual model, based on relevant information or reasonable inference from previous studies, we put forward the following hypothesis indicating causality: (1) Temperature and antecedent temperature conditions can affect the dynamic changes in vegetation (Nearing et al., 2005). (2) Both precipitation and antecedent precipitation can promote the increase of runoff; precipitation also has an indirect effect on runoff by changing vegetation dynamics (Peng and Wang, 2012; Li et al.,

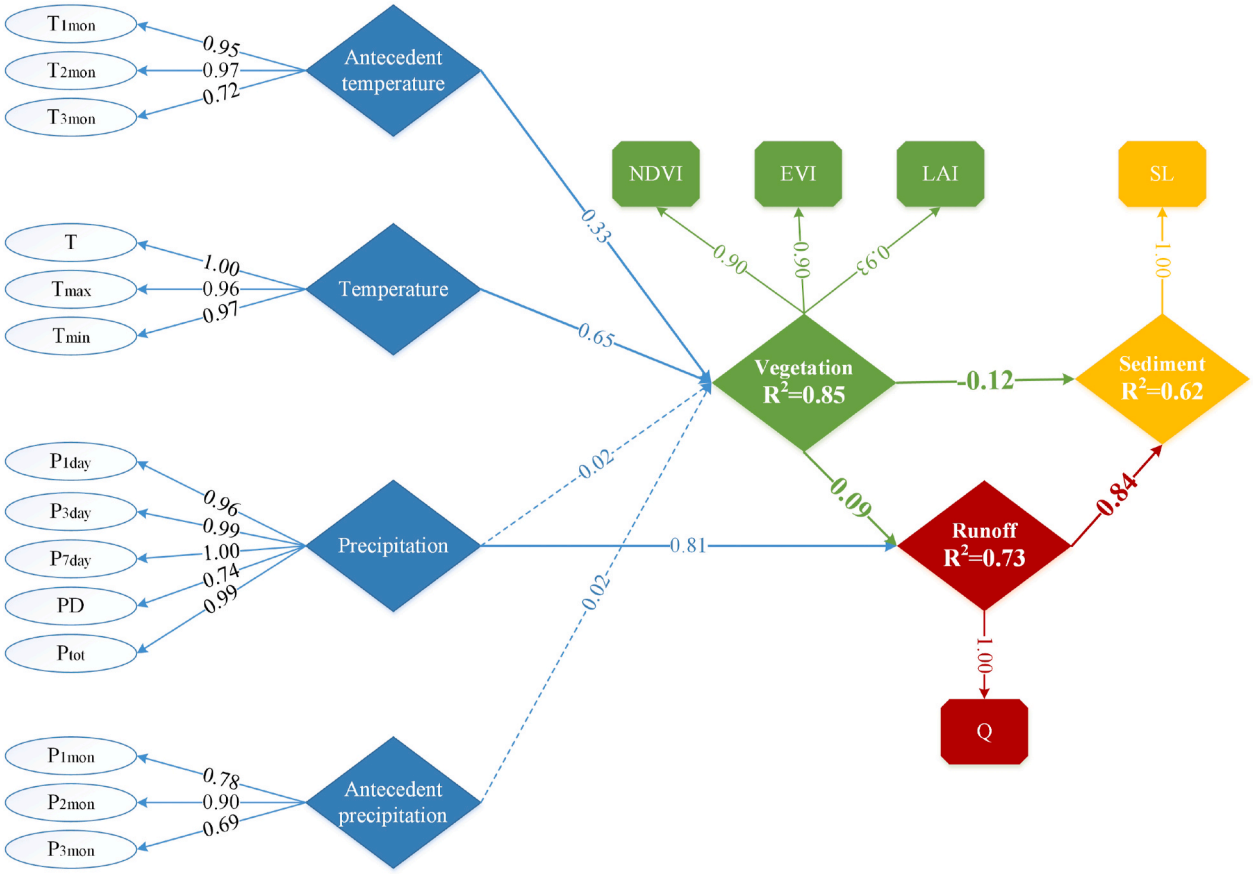

Fig. 7. Results of the PLS-SEM analysis. The number on the arrow between the potential variable and its observed variables represents the load. The bold arrows between latent variables indicate significant correlation ($P < 0.05$), and the numbers on the arrows represent path coefficients. The dashed arrows show nonsignificant relationships ($P > 0.05$). Abbreviations for the variables are listed in Table 1.

Table 5
Direct and indirect impacts, calculated using standardized path coefficients.

Latent Variables	Direct impact	Indirect impact	Total
Runoff			
Antecedent Temperature	N.A.	0.028	0.028
Temperature	N.A.	0.056	0.056
Antecedent Precipitation	N.A.	0.002	0.002
Precipitation	0.806	0.002	0.808
Vegetation	0.086	N.A.	0.086
Sediment Load			
Antecedent Temperature	N.A.	−0.015	−0.015
Temperature	N.A.	−0.030	−0.030
Antecedent Precipitation	N.A.	−0.001	−0.001
Precipitation	N.A.	0.672	0.672
Vegetation	−0.118	0.072	−0.046
runoff	0.835	N.A.	0.835
Vegetation			
Antecedent Temperature	0.328	N.A.	0.328
Temperature	0.652	N.A.	0.652
Antecedent Precipitation	0.023	N.A.	0.023
Precipitation	0.019	N.A.	0.019

N.A: It was not possible to determine direct or indirect effects.

2016). (3) Vegetation cover can affect the surface runoff; thus protecting soil indirectly affects sediment load change. Vegetation dynamics have a negative correlation with runoff and sediment load changes (Peng and Wang, 2012; Zhang et al., 2019). (4) Surface runoff directly affects the sediment load, and there is a positive correlation between the two (Zhao et al., 2015).

This study utilized a composition-based PLS-SEM model (Lohmoller, 2010). Through the combination of the measurement and structural models, the observed variables were connected with their corresponding latent variables, and the relationship between the latent variables was calculated. PLS-SEM analysis was conducted using R and a "PLSPM" software package.

3. Results

3.1. Temporal variation in monthly sediment load and its potential influencing factors

Table 2 provides descriptive statistics for monthly sediment load and its potential driving factors in the Liujiang watershed from 2003 to 2017. For the hydrological characteristics, the monthly runoff varied from 4.8 billion to 146 billion $m^3\ s^{-1}$, and the monthly sediment load ranged from 0 to 731 × 10^4 t, both of which showed high variability (coefficient of variation (CV) > 100%). Precipitation, temperature, and vegetation variables all demonstrated moderate variation, with the CV values ranging from 16.7% to 72.8%. Thus, monthly sediment load generally exhibited greater variability than its potential influencing factors. The monthly runoff and sediment load usually peaked yearly in June or July (Fig. 2). They both exhibited an increasing trend over the course of the study period, but the increase in the monthly sediment load was more significant (Table 3). The monthly runoff increased significantly in October and December ($P < 0.01$), while the monthly sediment load increased significantly in February, March, August, October, and December ($P < 0.01$, Table 3).

Fig. 3 shows the differences in runoff and sediment load among different months from 2003 to 2017; the two have obvious seasonal changes. The maximum monthly runoff was observed in June, but the

maximum monthly sediment load was generally detected in June and July. Similarly, the monthly mean, maximum, and minimum temperatures were highest during July–August, June–August and August, respectively (Table 4). The total monthly precipitation and maximum monthly 7-day precipitation were both significantly higher in June, and the maximum monthly 1-day and 3-day precipitation were highest in May and June, respectively. The number of >0.1 mm precipitation days was significantly higher in March–June. For the vegetation variables, the NDVI, EVI, and LAI were significantly higher in July–October, July–August, and July–September, respectively, than in other months ($P < 0.05$).

3.2. Selection of the factors influencing monthly sediment load

Figs. 4a and 5 show the correlation coefficient between vegetation index and temperature at different lag times (lag of 0, 1, 2, and 3 months, or T0, T1, T2, and T3, respectively). In most cases, the temperature significantly affected the vegetation index. Significant relationships were observed between NDVI and all lag times (T0–T3) ($P < 0.05$); the strongest correlation was with the temperature of the previous month (T1). Both EVI and LAI were significantly correlated with temperature for T0-T2 ($P < 0.05$), but no significant relationships were detected for T3 ($P > 0.05$). The strongest correlation between EVI, LAI, and temperature was observed for T0.

Fig. 4b shows the correlation coefficient between the vegetation index and precipitation at different lag times. The three vegetation indices were all significantly correlated with precipitation at all four lag times ($P < 0.05$). Among these, the strongest correlation between NDVI, LAI, and precipitation occurred for T2 (Fig. 6). For EVI, the strongest correlation was with the precipitation amount of the previous month (T1). The correlation between vegetation index and climate was significant at a lag time of 3 months; therefore, this was the appropriate time delay for vegetation index responses to climate.

3.3. PLS-SEM

Based on the monthly temperature, precipitation, vegetation index, and runoff data of the Liujiang watershed from 2003 to 2017, PLS-SEM was used to disentangle the impacts of climate and vegetation change on monthly sediment load. For the established PLS-SEM model, the *GOF* was 0.73 (>0.50), indicating that the model was effective (Tenenhaus et al., 2005). The values on the arrows in Fig. 7 represent the path coefficients (β) of the direct effect between the two variables. Both temperature and antecedent temperature had significant direct effects ($P < 0.01$) on vegetation dynamics ($\beta = 0.65$ and 0.33, respectively). Precipitation directly affected runoff and vegetation dynamics ($\beta = 0.81$ and 0.02, respectively). Runoff had a significant direct effect ($P < 0.01$) on sediment load ($\beta = 0.84$), but vegetation had significant opposite effects ($P < 0.05$) on runoff ($\beta = 0.09$) and sediment load ($\beta = -0.12$). Overall, climatic factors explained up to 85% of the monthly vegetation dynamics. Vegetation dynamics and climatic factors together explained 73% of the monthly runoff changes. Further, vegetation dynamics, climatic factors, and runoff accounted for 62% of the monthly sediment load changes.

Table 5 shows the influence results for all the variables in the PLS-SEM model, including direct, indirect, and total impacts. The total effect of precipitation on runoff (0.81) was greater than that of vegetation coverage (0.09) and temperature (0.06). The main driving factor of vegetation dynamics was temperature (0.65), and the least influential variable was precipitation (0.02). Runoff had the greatest influence on monthly sediment load (0.84), which was mainly a direct impact; this was followed by the total effects of precipitation (0.67), vegetation dynamics (−0.05), temperature (−0.03), antecedent temperature (−0.02), and antecedent precipitation (−0.01). The overall effect of vegetation dynamics on sediment load change was negative (−0.05); the direct effect (−0.12) was greater than the indirect effect (0.07). The total effect of vegetation dynamics on runoff (0.09) was greater than that on sediment load (−0.05).

4. Discussion

In the current study, PLS-SEM was selected to clarify the complex relationships among monthly sediment load and its potential influencing factors. Among them, climate change greatly affected plant biomass. Temperature had the most significant direct effect on vegetation dynamics ($\beta = 0.65$), and the antecedent temperature also had notable direct influence on vegetation ($\beta = 0.33$) (Table 5 and Fig. 7). Notably, temperature changes affect the amount and rate of plant biomass production in complex ways (Nearing et al., 2005). Moreover, temperature and antecedent temperature have a significant direct influence on the changes in vegetation. However, the direct influence of precipitation and antecedent precipitation on vegetation dynamics was non-significant ($P > 0.05$; Fig. 7). Precipitation and antecedent precipitation affect vegetation by replenishing soil water (Seeger et al., 2004; Peng and Wang, 2012; Li et al., 2016). Previous studies have shown that photosynthetic capacity increased with an increase in temperature, and generally had the optimum temperatures in the range of 30–40 °C (Kattge and Knorr, 2007; Lloyd and Farquhar, 2008; Huang et al., 2019). Climate change may alter this photosynthetic capacity and hence vegetation by increasing temperature frequencies beyond the thermal optimum for primary productivity of ecosystems (Bennett et al., 2021). Precipitation is abundant in the karst areas in southwest China; therefore, the temperature, rather than precipitation, is the limiting factor for vegetation dynamics.

Climatic factors can also strongly influence runoff changes. The influence of temperature and antecedent temperature on runoff was mainly indirect, while the direct influence of precipitation on runoff reached $\beta = 0.81$ (Table 5). However, increased temperature led to increased evapotranspiration and, thus, considerably affected vegetation dynamics. As a result, temperature indirectly influences runoff by affecting the vegetation (Seneviratne et al., 2010). In contrast, precipitation has a significant direct impact on runoff (Li et al., 2016). Generally, karst watersheds have poor water storage capacity, and precipitation contributes greatly to the changes in runoff. Precipitation and antecedent precipitation also affect plant growth through the soil water supply and further change runoff in the watershed by affecting surface interception and water evaporation (Seeger et al., 2004; Peng and Wang, 2012; Li et al., 2016).

However, the relationship between vegetation and runoff showed an unexpected positive correlation. Generally, vegetation preserves soil and water by trapping water and reducing erosion. Thus, previous studies observed a negative correlation between vegetation and annual runoff (Marques et al., 2007; Wei et al., 2007; Peng and Wang, 2012; Liang et al., 2015; Zhang et al., 2019). At the monthly scale, the climate characteristics in this watershed caused heavy precipitation to coincide with the times of highest vegetation coverage. As a result, high runoff happened mainly during the growing season, which generally corresponded to high vegetation coverage. Furthermore, in karst watersheds, precipitation generally causes a continuous increase in water in the underlying soil-epikarst system. When this system becomes saturated, surface runoff increases (Seeger et al., 2004; Peng and Wang, 2012; Li et al., 2016, 2017b). Hence, the effect of vegetation on runoff dynamics is largely regulated by the ability of the soil-epikarst system to store precipitation (Seeger et al., 2004).

The runoff, climatic factors, and vegetation characteristics were closely related to the large variability in the monthly sediment load (Knapen et al., 2007; Ouyang et al., 2010). Monthly sediment load was positively correlated with runoff (Fig. 7), which is consistent with previous studies (Zhao et al., 2015; Li et al., 2017b). Precipitation is also an important variable that controls the sediment load in karst watersheds and can cause soil erosion (Pruski and Nearing, 2002; Peng and Wang, 2012; Wang et al., 2015; Li et al., 2017b, 2018; Vercruysse et al., 2017).

In contrast, the direct (−0.12) and indirect (0.07) influence of vegetation on monthly sediment load were both relatively low. Generally, karst areas are mainly composed of highly soluble carbonate rocks, with physical and chemical properties that result in a low soil formation rate (Feng et al., 2014; Jiang et al., 2014). Additionally, a network of pores, fractures, and dissolution pipelines pervades karst aquifers, resulting in relatively complex and unique hydrogeological conditions (Hartmann et al., 2014; Wu et al., 2017), which allow large amounts of precipitation to be rapidly drained into underground rivers; this recharges the groundwater system and prevent the formation of surface runoff. The ratio of surface runoff to precipitation in karst areas is much lower than that in non-karst areas due to permeability (Hartmann et al., 2014; Jiang et al., 2014; Li et al., 2017c). Most of the sediment is transported to underground rivers, where it is deposited, or stored in underground karst environments, and relatively little sediment is transported by surface runoff (Jiang et al., 2014; Wu et al., 2017). Therefore, this special hydrogeology and geomorphology may reduce the direct influence of vegetation on monthly sediment load. Similarly, the indirect effect of vegetation on monthly sediment load by reducing surface runoff is also limited (Li et al., 2016). In contrast, consider non-karst areas, such as the Loess Plateau, where the vegetation coverage was relatively low prior to 1999. After large-scale vegetation rehabilitation programs, such as "Grain for Green" project, were implemented in 1999, the vegetation coverage significantly increased from 31.6% in 1999 to 59.6% in 2013 (Chen et al., 2015). Previous studies have shown that the substantial impact of vegetation on sediment load reduction can even exceed that of dam construction in these areas (Knapen et al., 2007; Wang et al., 2015). However, the vegetation coverage throughout southwest China has been relatively high in recent decades and has reached more than 80% (Tong et al., 2017). Recently, ecological engineering measures have also increased the vegetation coverage in the karst areas of southwest China. However, the inter-annual change has not been significant, and the increase rate was much smaller than in non-karst areas, such as the Loess Plateau. As a result, the effects of vegetation on monthly sediment load are limited to sections with relatively high vegetation coverage in karst areas. Therefore, the hydrogeological conditions coupled with a relatively high vegetation coverage rate can mediate the relationship between the vegetation and monthly sediment load variation in karst areas.

5. Conclusions

As one of the largest contiguous karst landscapes in the world, southwest China is an ecologically fragile area experiencing serious soil erosion, which was greatly influenced by climate variability and vegetation dynamics. Few studies have decoupled the influences of individual driving factor on monthly sediment load, as well interactive effects among driving factors in karst areas. This study utilized PLS-SEM to decouple the effects of climate and vegetation changes on monthly sediment load in a karst watershed of southwest china. Climatic factors had a direct impact on vegetation dynamics; among them, temperature had the most significant impact. Precipitation was the most significant direct factor for runoff changes, while temperature was the most significant indirect factor. Among the factors influencing sediment load change, the direct effect of runoff was the largest, and the indirect effect of precipitation was the most significant. The direct and indirect effects of vegetation on sediment load were both relatively limited. Runoff and precipitation were both positively correlated with the monthly sediment load, while antecedent temperature, temperature, antecedent precipitation, and vegetation dynamics were all negatively correlated with sediment load. This study provides a convenient and practical method to evaluate the coupling relationship between predicted latent factors and observed variables at the watershed scale. The result is helpful for the improvement of sediment yield predictions and yields a more in-depth understanding of the driving mechanisms of soil erosion in karst watersheds. It also provides a scientific basis for the development of a water resources management plan and reduction of soil loss under future climate change scenarios for the karst watershed.

CRediT authorship contribution statement

Si Cheng: Methodology, Data curation, Validation, Writing – original draft. **Xingxiu Yu:** Conceptualization, Writing – review & editing. **Zhenwei Li:** Data curation, Supervision, the research and, Co-wrote the paper. **Xianli Xu:** Writing – review & editing. **Huayi Gao:** Writing – review & editing. **Zongda Ye:** Writing – review & editing.

Declaration of competing interest

The authors declare that they have no known competing financial interests or personal relationships that could have appeared to influence the work reported in this paper.

Data availability

The data that has been used is confidential.

Acknowledgments

This study was supported by the State Key Program of the National Natural Science Foundation of China (41730748), National Natural Science Foundation of China (41977073), National Key Research and Development Program of China (2019YFE0116900), Youth Innovation Promotion Association of CAS (2020359), the Science and Technology Innovation Program of Hunan Province (2021RC3115), and Natural Science Foundation of Hunan Province (2022JJ30646).

References

Anderson, L.O., Malhi, Y., Araga, L.E.O.C., Ladle, R., Arai, E., Barbier, N., Phillips, O., 2010. Remote sensing detection of droughts in Amazonian forest canopies. New Phytol. 187, 733–750.

Bennett, A.C., Arndt, S.K., Bennett, L.T., Knauer, J., Beringer, J., Griebel, A., HinkoNajera, N., Liddell, M.J., Metzen, D., Pendall, E., Silberstein, R.P., Wardlaw, T. J., Woodgate, W., Haverd, V., 2021. Thermal optima of gross primary productivity are closely aligned with mean air temperatures across Australian wooded ecosystems. Global Change Biol. 27 (19), 4727–4744.

Borrelli, P., Robinson, D.A., Panagos, P., Lugato, E., Yang, J.E., Alewell, C., Wuepper, D., Montanarella, L., Ballabio, C., 2020. Land use and climate change impacts on global soil erosion by water (2015-2070). Proc. Natl. Acad. Sci. USA 117, 1–8.

Chen, X.Q., Zong, Y.Q., Zhang, E.F., Xu, J.G., Li, S.J., 2001. Human impacts on the Changjiang Yangtze River basin, China, with special reference to the impacts on the dry season water discharges into the sea. Geomorphology 41, 111–123.

Chen, L.D., Messing, I., Zhang, S.R., Fu, B.J., Ledin, S., 2003. Land use evaluation and scenario analysis towards sustainable planning on the Loess Plateau in China-case study in a small catchment. Catena 54, 303–316.

Chen, T., Jeu, R.D., Liu, Y.Y., Werf, G.V.D., Dolman, A.J., 2014. Using satellite based soil moisture to quantify the water driven variability in ndvi: a case study over mainland Australia. Remote Sensing of Environment 140, 330–338.

Chen, Y.P., Wang, K.B., Lin, Y.S., Shi, W.Y., Song, Y., He, X.H., 2015. Balancing green and grain trade. Nat. Geosci. 8 (10), 739–741.

Feng, T., Chen, H.S., Wang, K.L., Zhang, W., Qi, X.K., 2014. Modeling soil erosion using a spatially distributed model in a karst catchment of northwest guangxi, China. Earth Surf. Process. Landforms 39, 2121–2130.

Feng, X.M., Cheng, W., Fu, B.J., Lue, Y.H., 2016. The role of climatic and anthropogenic stresses on long-term runoff reduction from the loess plateau, China. Sci. Total Environ. 571, 688–698.

Gao, G.Y., Zhang, J.J., Liu, Y., Ning, Z., Fu, B.J., Sivapalan, M., 2017. Spatio-temporal patterns of the effects of precipitation variability and land use/cover changes on long-term changes in sediment yield in the Loess Plateau, China. Hydrol. Earth Syst. Sci. 21 (9), 4363–4378.

Gao, Z.L., Fu, Y.L., Li, Y.H., Liu, J.X., Chen, N., Zhang, X.P., 2012. Trends of streamflow, sediment load and their dynamic relations for the catchments in the middle reaches of the Yellow River in the past five decades. Hydrol. Earth Syst. Sci. 16 (9), 3219–3231.

Grace, J.B., Schoolmaster, D.R., Guntenspergen, G.R., Little, A.M., Mitchell, B.R., Miller, K.M., Schweiger, E.W., 2012. Guidelines for a graph-theoretic implementation of structural equation modeling. Ecosphere 3 (8), 73.

Hartmann, A., Goldscheider, N., Wagener, T., Lange, J., Weiler, M., 2014. Karst water resources in a changing world: review of hydrological modeling approaches. Rev. Geophys. 52 (3), 218–242.

Huang, M., Piao, S.L., Ciais, P., Peñuelas, J., Wang, X.H., Keenan, T.F., Peng, S.S., Berry, J.A., Wang, K., Mao, J.F., Alkama, R., Cescatti, A., Cuntz, M., De, D.H., Gao, M.D., He, Y., Liu, Y.W., Luo, Y.Q., Myneni, R.B., Niu, S.L., Shi, X.Y., Yuan, W.P., Verbeeck, H., Wang, T., Wu, J., Janssens, I.A., 2019. Air temperature optima of vegetation productivity across global biomes. Nature Ecology & Evolution 3 (5), 772–779.
Jiang, Z.C., Lian, Y.Q., Qin, X.Q., 2014. Rocky desertification in Southwest China: impacts, causes, and restoration. Earth Sci. Rev. 132, 1–12.
Kattge, J., Knorr, W., 2007. Temperature acclimation in a biochemical model of photosynthesis: a reanalysis of data from 36 species. Plant Cell Environ. 30 (9), 1176–1190.
Knapen, A., Poesen, J., Govers, G., Gyssels, G., Nachtergaele, J., 2007. Resistance of soils to concentrated flow erosion: a review. Earth Sci. Rev. 80 (1–2), 75–109.
Li, Z.W., Zhang, G.H., Geng, R., Wang, H., Zhang, X.C., 2015. Land use impacts on soil detachment capacity by overland flow in the loess plateau, China. Catena 124, 9–17.
Li, Z.W., Xu, X.L., Yu, B.F., Xu, C.H., Liu, M.X., Wang, K.L., 2016. Quantifying the impacts of climate and human activities on water and sediment discharge in a karst region of southwest China. J. Hydrol. 542, 836–849.
Li, Z.W., Xu, X.L., Liu, M.X., Li, X.Z., Zhang, R.F., Wang, K.L., Xu, C.H., 2017a. State-space prediction of spring discharge in a karst catchment in southwest China. J. Hydrol. 549, 264–276.
Li, Z.W., Xu, X.L., Xu, C.H., Liu, M.X., Yi, R.Z., 2017b. Monthly sediment discharge changes and estimates in a typical karst catchment of southwest China. J. Hydrol. 555, 99–107.
Li, Z.W., Xu, X.L., Xu, C.H., Liu, M.X., Wang, K.L., Yu, B.F., 2017c. Annual runoff is highly linked to precipitation extremes in karst catchments of southwest China. J. Hydrol. 10, 2745–2759.
Li, Z.W., Xu, X.L., Xu, C.H., Liu, M.X., Wang, K.L., 2018. Dam construction impacts on multiscale characterization of sediment discharge in two typical karst watersheds of southwest China. J. Hydrol. 558, 42–54.
Li, Z.W., Xu, X.L., Zhang, Y.H., Wang, K.L., Zeng, P., 2019. Reconstructing recent changes in sediment yields from a typical karst watershed in southwest China. Agric. Ecosyst. Environ. 269, 62–70.
Liang, W., Bai, D., Wang, F.Y., Fu, B.J., Yan, J.P., Wang, S., Yang, Y.T., Long, D., Feng, M. Q., 2015. Quantifying the impacts of climate change and ecological restoration on streamflow changes based on a Budyko hydrological model in China's Loess Plateau. Water Resour. Res. 51, 6500–6519.
Lin, G.H., Phillips, S.L., Ehleringer, J.R., 1996. Monosoonal precipitation responses of shrubs in a cold desert community on the Colorado plateau. Oecologia 106 (1), 8–17.
Liu, M., Bai, X.Y., Tan, Q., Luo, G.J., Zhao, C.W., Wu, L.H., Luo, X.L., Ran, C., Zhang, S.R., 2022. Climate change enhances the positive contribution of human activities to vegetation restoration in China. Geocarto Int. 1–24.
Lloyd, J., Farquhar, G.D., 2008. Effects of rising temperatures and [CO_2] on the physiology of tropical forest trees. Phil. Trans. Biol. Sci. 363 (1498), 1811–1817.
Lohmoller, J.B., 2010. The pls program system: latent variables path analysis with partial least squares estimation. Multivariate Behav. Res. 23 (1), 125–127.
Marques, M.J., Bienes, R., Jimenez, L., Perez-Rodriguez, R., 2007. Effect of vegetal cover on runoff and soil erosion under light intensity events. Rainfall simulation over USLE plots. Sci. Total Environ. 378 (1–2), 161–165.
Miao, C.Y., Ni, J.R., Borthwick, A.G.L., Yang, L., 2011. A preliminary estimate of human and natural contributions to the changes in water discharge and sediment load in the Yellow River. Global Planet. Change 76 (3–4), 196–205.
Mwangi, H.M., Julich, S., Patil, S.D., Mcdonald, M.A., Feger, K.H., 2016. Relative contribution of land use change and climate variability on discharge of upper mara river, Kenya. Journal of Hydrology Regional Studies 5 (1), 244–260.
Nearing, M.A., Jetten, V., Baffautc, C., Cerdand, O., Couturierd, A., Hernandeza, M., Bissonnaise, Y.L., Nicholsa, M.H., Nunesf, J.P., Renschlerg, C.S., Souchèreh, V., Oosti, V., 2005. Modeling response of soil erosion and runoff to changes in precipitation and cover. Catena 61 (2–3), 131–154.
OuYang, W., Hao, F.H., Skidmore, A.K., Toxopeus, A.G., 2010. Soil erosion and sediment yield and their relationships with vegetation cover in upper stream of the yellow river. Sci. Total Environ. 409 (2), 396–403.
Pearl, J., 2012. The causal mediation formula-a guide to the assessment of pathways and mechanisms. Prev. Sci. 13, 426–436.
Peng, T., Wang, S.J., 2012. Effects of land use, land cover and rainfall regimes on the surface runoff and soil loss on karst slopes in southwest China. Catena 90 (1), 53–62.
Pruski, F.F., Nearing, M.A., 2002. Climate-induced changes in erosion during the 21st century for eight U.S. locations. Water Resour. Res. 38 (12), 1298.
Rundquist, B.C., Harrington Jr., J.A., 2000. The effects of climatic factors on vegetation dynamics of tallgrass and shortgrass cover. Geocarto Int. 15 (3), 33–38.
Saatchi, S., Asefi-Najafabady, S., Malhi, Y., Aragão d, L.E.O.C., Andersonc, L.O., Mynenif, R.B., Nemanig, R., 2013. Persistent effects of a severe drought on amazonian forest canopy. Proc. Natl. Acad. Sci. USA 110 (2), 565–570.
Seeger, M., Erreab, M.P., Begueria, S., Arnaez, J., Marti, C., Garcia-Ruiz, J.M., 2004. Catchment soil moisture and rainfall characteristics as determinant factors for discharge/suspended sediment hysteretic loops in a small headwater catchment in the Spanish pyrenees. J. Hydrol. 288 (3–4), 299–311.
Seneviratne, S.I., Corti, T., Davin, E.L., Hirschi, M., Jaeger, E.B., Lehner, I., Orlowsky, B., Teuling, A.J., 2010. Investigating soil moisture-climate interactions in a changing climate: a review. Earth Sci. Rev. 99 (3–4), 125–161.
Serpa, D., Nunes, J.P., Santos, J., Sampaio, E., Jacinto, R., Veiga, S., Lima, J.C., Moreira, M., Corte-Real, J., Keizer, J.J., Abrantes, N., 2015. Impacts of climate and land use changes on the hydrological and erosion processes of two contrasting mediterranean catchments. Sci. Total Environ. 538, 64–77.
Shi, Z.H., Huang, X.D., Ai, L., Fang, N.F., Wu, G.L., 2014. Quantitative analysis of factors controlling sediment yield in mountainous watersheds. Geomorphology 226, 193–201.
Sivapalan, M., Kumar, P., Harris, D., 2001. Nonlinear propagation of multi-scale dynamics through hydrologic subsystems. Adv. Water Resour. 24, 935–940.
Syvitski, J.P.M., Voeroesmarty, C.J., Kettner, A.J., Green, P., 2005. Impact of humans on the flux of terrestrial sediment to the global coastal ocean. Science 308 (5720), 376–380.
Tenenhaus, M., Vinzi, V.E., Chatelin, Y.M., Lauro, C., 2005. Pls path modeling. Comput. Stat. Data Anal. 48, 159–205.
Tenenhaus, M., 2008. Component-based structural equation modelling. Total Qual. Manag. Bus. Excel. 19 (7–8), 871–886.
Tong, X.W., Wang, K.L., Yue, Y.M., Brandt, L., Liu, B., Zhang, C.H., Liao, C.J., Fensholt, R., 2017. Quantifying the effectiveness of ecological restoration projects on long-term vegetation dynamics in the karst regions of southwest China. Int. J. Appl. Earth Obs. Geoinf. 54, 105–113.
Vercruysse, K., Grabowski, R.C., Rickson, R.J., 2017. Suspended sediment transport dynamics in rivers: multi-scale drivers of temporal variation. Earth Sci. Rev. 166, 38–52.
Vinzi, V.E., Trinchera, L., Amato, S., 2010. Pls Path Modeling: from Foundations to Recent Developments and Open Issues for Model Assessment and Improvement. Springer Berlin Heidelberg, pp. 47–82.
Wang, S., Fu, B.J., Piao, S.L., Lü, Y.H., Ciais, P., Feng, X.M., Wang, Y.F., 2015. Reduced sediment transport in the Yellow River due to anthropogenic changes. Nat. Geosci. 9 (1), 38–41.
Wang, F., Mu, X.M., Hessel, R., Zhang, W., Ritsema, C.J., Li, R., 2013. Runoff and Sediment load of the Yan River, China: changes over the last 60 yr. Hydrol. Earth Syst. Sci. 17 (7), 2515–2527.
Wei, W., Chen, L.D., Fu, B.J., Huang, Z.L., Wu, D.P., Gui, L.D., 2007. The effect of land uses and rainfall regimes on runoff and soil erosion in the semi-arid loess hilly area, China. J. Hydrol. 335 (3–4), 247–258.
Wu, D.H., Zhao, X., Liang, S.L., Zhou, T., Huang, K.C., Tang, B.J., Zhao, W.Q., 2015. Time-lag effects of global vegetation responses to climate change. Global Change Biol. 9, 3520–3531.
Wu, L.H., Wang, S.J., Bai, X.Y., Luo, W.J., Tian, Y.C., Zeng, C., Luo, G.J., He, S.Y., 2017. Quantitative assessment of the impacts of climate change and human activities on runoff change in a typical karst watershed, SW China. Sci. Total Environ. 601–602, 1449–1465.
Xu, X.L., Ma, K.M., Fu, B.J., Song, C.J., Liu, W., 2008. Influence of three plant species with different morphologies on water runoff and soil loss in a dry-warm river valley, SW China. For. Ecol. Manag. 256 (4), 656–663.
Yan, D., Schneider, U.A., Schmid, E., Huang, H.Q., Pan, L.H., Dilly, O., 2013. Interactions between land use change, regional development, and climate change in the poyang lake district from 1985 to 2035. Agric. Syst. 119, 10–21.
Zhang, S.R., Lu, X.X., 2009. Hydrological responses to precipitation variation and diverse human activities in a mountainous tributary of the lower Xijiang, China. Catena 77 (2), 130–142.
Zhang, S.R., Bai, X.Y., Zhao, C.W., Tan, Q., Luo, G.J., Cao, Y., Deng, Y.H., Li, Q., Li, C.J., Wu, L.H., Wang, J.F., Chen, F., Xi, H.P., Ran, C., Liu, M., 2021. Limitations of soil moisture and formation rate on vegetation growth in karst areas. Sci. Total Environ. 6, 151209.
Zhang, Z.C., Chen, X., Huang, Y.Y., Zhang, Y.F., 2014. Effect of catchment properties on runoff coefficient in a karst area of southwest China. Hydrol. Process. 28 (11), 1–12.
Zhang, S.H., Li, Z.H., Hou, X.N., Yi, Y.J., 2019. Impacts on watershed-scale runoff and sediment yield resulting from synergetic changes in climate and vegetation. Catena 179, 129–138.
Zhao, F.F., Zhang, L., Xu, Z.X., Scott, D.F., 2010. Evaluation of methods for estimating the effects of vegetation change and climate variability on streamflow. Water Resour. Res. 46 (3), 742–750.
Zhao, Y.F., Zou, X.Q., Gao, J.H., Xu, X.W.H., Wang, C.L., Tang, D.H., Wang, T., Wu, X.W., 2015. Quantifying the anthropogenic and climatic contributions to changes in water discharge and sediment load into the sea: a case study of the Yangtze River, China. dec.1 Sci. Total Environ. 536, 803–812.
Zhou, G.Y., Wei, X.H., Chen, X.Z., Zhou, P., Liu, X.D., Xiao, Y., Sun, G., Scott, D.F., Zhou, S.Y.D., Han, L.S., Su, Y.X., 2015. Global pattern for the effect of climate and land cover on water yield. Nat. Commun. 23 (3), 40.